



DECLASSIFIED

3

REF.
DEPT.

**AUSTRALIAN ATOMIC ENERGY COMMISSION
RESEARCH ESTABLISHMENT
LUCAS HEIGHTS**

**FISSION PRODUCT RETENTION OF FUELLED BERYLLIUM OXIDE SPHERES
AND URANIA-THORIA FUEL PARTICLES IN POST-IRRADIATION
ANNEALING EXPERIMENTS**

by

**D. ROMAN
C.H. RANDALL
G.L. HANNA**

December 1969 **DECLASSIFIED**

AUSTRALIAN ATOMIC ENERGY COMMISSION
RESEARCH ESTABLISHMENT
LUCAS HEIGHTS

FISSION PRODUCT RETENTION OF FUELLED BERYLLIUM
OXIDE SPHERES AND URANIA-THORIA FUEL PARTICLES
IN POST-IRRADIATION ANNEALING EXPERIMENTS

by

D. ROMAN
C. H. RANDALL
G. L. HANNA

ABSTRACT

The post-activation diffusion technique has been used to measure the release of Xe-133 from beryllium oxide based, spherical fuel elements and the urania-thoria fuel particles from which they were prepared. Release rate parameters (apparent diffusion coefficients, D') for bare fuel particles were of the order 10^{-8} sec^{-1} to $10^{-10} \text{ sec}^{-1}$ at 1400°C , whereas most spheres tested gave parameters of $10^{-16} \text{ sec}^{-1}$ or less, indicating that the beryllia matrix and cladding were having a marked effect in retaining fission gases.

Mid-anneal changes in release rates from bare fuel particles were observed at 1200°C and 1400°C . This behaviour is tentatively attributed to slight pore growth and the release of trapped gas from pores which open to the surface during annealing.

CONTENTS

	Page
1. INTRODUCTION	1
2. EXPERIMENTAL TECHNIQUE	1
2.1 General Features of Experimental Method	1
2.2 Details of Experimental Method	2
3. XENON RELEASE FROM FUEL PARTICLES	3
3.1 Specimen Details	3
3.2 Release of Xe-133	3
3.3 Summary of Results on Fuel Particles	5
4. XENON RELEASE FROM PROTOTYPE FUEL ELEMENTS	6
4.1 Specimen Details	6
4.2 Release of Xe-133	6
5. DISCUSSION	7
6. CONCLUSIONS	7
7. REFERENCES	8

Table 1 Summary of Xe-133 Release Parameters and Fabrication Histories for Urania-Thoria Fuel Particles

Table 2 Summary of Xe-133 Release Parameters for Prototype BeO Based Fuel Elements for the ABORIGINE Reactor

Figure 1 Diagram of Apparatus for Post-activation Diffusion Experiments

Figure 2 Diffusion Curve for COP-25-B2 Fuel Particles at 1000 °C

Figure 3 Diffusion Curve for COP-25-B2 Fuel Particles at 1400 °C

Figure 4 Arrhenius Plots of Release Parameters obtained for Fuel Particles

Figure 5 Diffusion Curve for Fuel Particles, showing a Mid-anneal 'Burst'

Figure 6 Photomicrograph of Urania-Thoria Fuel Particles from Batch COP-25-B2

1. INTRODUCTION

The Australian Atomic Energy Commission has been studying a 200 kW(e) beryllia moderated, nuclear reactor known as ABORIGINE for which there are two conceptual adaptations of the basic design. One is an air-cooled system with an open cycle and the other a carbon dioxide cooled system with closed cycle. For both systems the fuel element must be capable of retaining fission products to a high degree so as to avoid hazardous contamination of the environment (open cycle) or the build-up of high levels of radioactivity in a closed cycle coolant circuit.

As part of the fabrication programme designed to improve the fission product retention properties of the ABORIGINE fuel element, the release of gaseous fission products has been measured using both in-pile and post-irradiation techniques. Attention was confined to the noble gases because these are convenient to handle experimentally and, with the radioiodines, are the most troublesome with regard to contamination of the coolant in a gas-cooled reactor. This report describes the post-irradiation experiments which, because of relative ease and cheapness, are better than in-pile experiments as sorting tests when several materials and many samples are available. The in-pile experiments, which were run in parallel but in smaller numbers, will be reported separately.

The ABORIGINE fuel element is a 1½ in. diameter sphere of beryllia (the moderator) fuelled with a solid solution of urania stabilised with thorium. The fuel is contained in a kernel as a dispersion in BeO, and this kernel is clad with an unfuelled layer of beryllia to retain fission products. The four stages in the development of this design were:

- (i) Coarse (200 micrometres) fuel particles of $\text{UO}_2\text{-ThO}_2$ solid solution dispersed in and bonded to a matrix of BeO. This fuelled kernel was surrounded by and bonded to an unfuelled outer shell of BeO about 1.5 mm thick.
- (ii) As in (i) but with the unfuelled outer shell increased in thickness to 4.6 mm and the kernel diameter reduced accordingly.
- (iii) As in (ii) but with fine (less than 10 micrometres) fuel particles.
- (iv) As in (iii) but with a porous friable BeO layer, about 0.7 mm thick, separating the kernel from the unfuelled shell.

The reasons for the change to fine fuel particles and the introduction of the porous BeO layer have been detailed by Walker and Hickman (1967) and Hickman et al. (1968). Compared with coarse fuel particles the fine particles improve mechanical properties both before and after irradiation, and the porous layer is designed to accommodate radiation-induced swelling of the kernel and to reduce β -particle bombardment of the BeO cladding.

Obviously, the fission product retention properties of such a fuel element are very dependent on those of the BeO. Hence, it was considered necessary to measure the fission product retention of both the bare fuel particles and the fabricated fuel elements in order to assess adequately the part played by the beryllium oxide. Fuel particles were incorporated into BeO matrixes by isostatic pressing followed by sintering at 1350 °C to 1575 °C, which was 125 °C to 350 °C below the sintering temperature of the fuel particles. Metallographic examination has shown that their characteristics do not change during this treatment. The xenon release measurements made on bare fuel particles and on the fuelled spheres are described separately.

The fuel particles and the spheres used in this programme were prepared at the Research Establishment by the Ceramics Group using techniques described by Reeve et al. (1966).

2. EXPERIMENTAL TECHNIQUE

2.1 General Features of Experimental Method

The post activation diffusion or P.A.D. method (Booth 1957) was used in which the specimen

is irradiated with neutrons at low temperature and then annealed at high temperature; the escaping radioactive gas (usually Xe-133 in low burnup work) is trapped and periodically assayed by gamma counting.

Data are usually interpreted in terms of the Equivalent Sphere Model (Booth 1957) which assumes that the specimen consists of an aggregate of small fully dense spheres with the same surface to volume ratio as the sample material and whose radius, a , is calculated from the B.E.T. surface area. Solution of the diffusion equation for these conditions gives the expression:

$$f = 6 \sqrt{D't/\pi} - 3D't$$

where f = fraction of total gas released at time t ,
 t = elapsed time since start of anneal
 D' = D/a^2 , the 'apparent' diffusion coefficient
 a = radius of equivalent sphere.

For practical annealing times the term $3D't$ is small enough ($D' \ll t^{-1}$) to be neglected and the expression reduces to:

$$f = 6 \sqrt{D't/\pi}$$

The curve of f plotted against \sqrt{t} should therefore be a straight line, from whose slope the apparent diffusion coefficient, D' can be calculated.

In this simple form the Equivalent Sphere Model is quite inadequate in any mechanistic sense because it does not take into account numerous factors such as pre-existing pores, grain boundaries, radiation-induced lattice defects, etc., which greatly affect the rate of transport of the migrating species. For this reason, diffusion coefficients evaluated by this method do not have any absolute significance. However, if care is taken to standardise the experimental conditions, they do have a useful relative significance which allows comparison of the potential of several materials as nuclear fuels. This is the only reason for the use of the Equivalent Sphere Model in this work, and D' is referred to as 'release rate parameter' or 'release parameter' rather than 'apparent diffusion coefficient'.

2.2 Details of Experimental Method

Specimens were irradiated in a neutron flux of about $5 \times 10^{12} \text{ n cm}^{-2} \text{ sec}^{-1}$ to a burnup of 3×10^{15} fissions per cm^3 in the fuel particles. Small cobalt monitors were irradiated with each specimen to permit accurate calculation of burnup. According to the findings of MacEwan and Stevens (1964) and Frigerio and Gerevini (1965) this should have been low enough to avoid burnup-dependent changes in the diffusion rates of Xe-133. Specimens were allowed to cool for five days or more before the post-activation anneals were commenced; this ensured that the I-133 precursor had decayed to Xe-133 and that accurate decay corrections for xenon could be made using the exponential decay law in its simplest form.

The P.A.D. apparatus is shown diagrammatically in Figure 1. The irradiated sample was contained in a platinum crucible and helium was passed through the system at about $60 \text{ cm}^3 \text{ min}^{-1}$. Xe-133 and other gaseous fission products escaping from the specimen were entrained in the stream and passed over a copper gauze trap at 300°C to remove radioiodines (mainly eight-day I-131) and thence to a charcoal trap maintained at -78°C in a dry ice-acetone bath. These traps, made of glass, fitted neatly and with reproducible geometry into the well of the sodium iodide scintillator used for gamma counting. Xenon traps were replaced periodically during a run and the total or cumulative activity release was determined by summation of the activity on individual traps.

Residual xenon contents were determined after the annealing runs by measuring the xenon evolved during chemical dissolution of the sample. Samples were placed in a flask connected to the helium line and thoroughly flushed to remove air. A 1:1 mixture of sulphuric and phosphoric acids was introduced to the flask, slowly brought to the boil, and held there until the specimen had dissolved. Released xenon was trapped and counted just as it was during the anneal but in order to cope with the large amount of activity and its rapid release during the dissolution, four traps were placed in circuit at any given time and the sweep gas was directed to the desired trap by a multi-way tap. Up to ten traps were sometimes used in one dissolution run.

Fuel particle samples could be submitted for dissolution immediately after annealing, but the fuelled spheres were cooled for a further 30 days because of their high Xe-133 content.

The total Xe-133 collected during the dissolution run was corrected for decay to the start of the P.A.D. run. Corrections were applied also for individual samples from the anneal to allow the amount escaping during any time interval to be expressed as a fraction of the total present in the specimen during that interval.

3. XENON RELEASE FROM FUEL PARTICLES

3.1 Specimen Details

All fuel particles tested were of the 'coarse' type, that is, about 200 microns in diameter; no measurements were made on finer particles. All particles consisted of a solid solution of UO_2 and ThO_2 with a nominal atom ratio of 1U:10Th.

The fluorite crystal structure of the UO_2 - ThO_2 solid solution is stable to high temperatures at this U:Th ratio. However, the oxygen content can vary in the range $(\text{U}_{0.1}, \text{Th}_{0.9})\text{O}_2$ to $(\text{U}_{0.1}, \text{Th}_{0.9})\text{O}_{2.045}$ (Cohen and Berman 1966) and this variation is accompanied by a colour change from green to dark grey. The procedure used to prepare the BeO-based fuel elements described in Section 4 involved a final sintering in unpurified nitrogen at 1300 °C to 1700 °C and this raised the oxygen content of the fuel particles to near the upper limit. Hence, in order that bare fuel particles could be tested in the same oxidation state as those in fuel elements, all fuel particles supplied for testing were oxidised in air at 800 °C before irradiation. Thus, it was considered unnecessary to purify the helium sweep gas by removing oxygen (already < 40 ppm) and moisture (< 20 ppm) for the P.A.D. anneals. It was assumed that the materials were fully oxidised and no direct measurements of oxygen-metal ratio were made.

Sample weights were 0.02 to 0.03 gram where possible but at one stage, when the reactor was scheduled to be shut down for a prolonged period, larger samples were used so that even after cooling for one month or more, the amounts of contained Xe-133 were adequate for measurement of release parameters.

Details of the materials are given in Table 1, together with summarised fabrication histories. In all, six batches of particles were tested. Batch COP-25-B2 was tested at four temperatures in the range 800 °C to 1400 °C, batch X-124-1,2 at 1400 °C, 1200 °C and 1000 °C, and the other four at 1200 °C only. The six batches differed slightly in U:Th ratio and fabrication history, and in one batch (X-124-3) the uranium contained was enriched to 20 per cent U-235.

3.2 Release of Xe-133

The diffusion curves usually reported for P.A.D. experiments are typified by the one in Figure 2 obtained with batch COP-25-B2 at 1000 °C. The initial non-linear or 'burst' portion of the curve quickly gives way to the linear region where the fractional release is proportional to the square root of the annealing time and from which the value of D' is calculated. However, it was found in this work that as the annealing temperature was increased, the linear portion of the plot showed a tendency to increase in slope after about 4 to 7 hours of annealing. Such a curve, obtained on COP-25-B2 at 1400 °C is shown in Figure 3; this result is typical of all runs at 1400 °C and some at 1200 °C, but at 1000 °C and 800 °C all results gave curves of the Figure 2 type.

The significance of this change in slope at high annealing temperatures is discussed below but, to compare values of release parameters, only the data obtained in the first 4 to 7 hours were used for the runs at higher temperature. Thus, all values for D' quoted in this report were obtained from the slope of either the sole or the first linear region.

Mean release parameters measured at 1200 °C on the several batches (see Table 1) were scattered over two orders of magnitude in the range $3.5 \times 10^{-9} \text{ sec}^{-1}$ to $9 \times 10^{-12} \text{ sec}^{-1}$. Furthermore, a comparison of the release parameters for batches COP-25-B2 and COP-17-B2A shows that, although they were prepared by nominally the same fabrication route, they gave respectively the lowest and highest results of all batches tested at 1200 °C. Hence, the difference observed with various fabrication routes might well have been due to the same factor (as yet unknown) which causes scatter in particles from a given fabrication batch; the differences cannot be ascribed with confidence to fabrication route changes.

Results obtained on batches COP-25-B2 and X-124-1,2 are shown in an Arrhenius plot in Figure 4. It appears that the energy of activation for the migration process remains constant over the range 1000 °C to 1400 °C but probably decreases below 1000 °C (see curve for COP-25-B2). The values $66,300 \text{ cal mole}^{-1}$ for COP-25-B2 above 1000 °C and $70,700 \text{ cal mole}^{-1}$ for X-124-1,2 compare well with the value $75,900 \text{ cal mole}^{-1}$ determined by Toner and Scott (1961) for $\text{ThO}_2 - 5 \text{ w/o UO}_2$ and with the higher values ($65,000 - 76,000 \text{ cal mole}^{-1}$) reported for Xe-133 in UO_2 and Kr85 in UO_2 (see Belle 1961 and Davies and Long 1963).

The Arrhenius equations determined for the two batches of fuel were:

$$\text{COP-25-B2} \quad D' = 0.058 e^{-66,300/RT}$$

$$\text{X-124-1,2} \quad D' = 3.573 e^{-70,700/RT}$$

Sufficient results were obtained on batches COP-25-B2 and X-124-1,2 to show that there was a genuine difference of about 10 times in their release parameters. This was probably due to differences in degree and distribution of porosity in the two materials. Batch X-124-1,2 had a higher measured bulk density than batch COP-25-B2, indicating a lower overall porosity. However, it also had a higher B.E.T. surface area ($0.032 \text{ m}^2 \text{ g}^{-1}$ compared to $0.0097 \text{ m}^2 \text{ g}^{-1}$) which, in view of their similar mesh size, suggested a higher degree of open porosity and a lower equivalent sphere diameter. High bulk density and high surface area are not compatible for a given mesh size and the measured values suggest that impregnation of open pores occurred during the measurement of density on the X-124-1,2 material. The surface areas quoted above yield equivalent sphere diameters of 70 microns for COP-25-B2 and 20 microns for X-124-1,2. Remembering that in terms of the Equivalent Sphere Model the 'true' diffusion coefficient, D (or D' for a fully dense sphere of unit radius) is related to the apparent diffusion coefficient by the expression $D' = D/a^2$, it is possible to calculate the values of D_0 (that is, the pre-exponential in the Arrhenius equation) for each material using these estimates of a . The values obtained are $D_0 = 3.57 \times 10^{-6} \text{ cm}^2 \text{ sec}^{-1}$ for X-124-1,2 and $D_0 = 1.07 \times 10^{-6} \text{ cm}^2 \text{ sec}^{-1}$ for COP-25-B2. These two values agree reasonably well, suggesting that the major difference in the behaviour of the two batches is the result of a difference in open porosity.

Another feature of the results which deserves attention is the mid-anneal changes in release rate at 1200 °C and 1400 °C as evidenced by the changes in slope of the f versus \sqrt{t} curves. The observed changes were of three types:

- i. From one linear region to a second linear region of greater slope which persisted for the remainder of the anneal (see Figure 3).
- ii. A sudden pronounced increase in slope followed by a return to the slope of the first linear region.
- iii. A sudden pronounced increase in slope followed by a second linear region of slope greater than that of the first linear region (see Figure 5).

These effects can possibly be explained by the release of trapped gas by the conversion of closed pores to open pores during the anneal. A burst may result from the rapid release of gas from a pore which opens directly to the free surface. Similarly, a prolonged or permanent increase in release rate might result from an internal pore opening into other interconnected pores (slow release to the surface) or by successive opening of many pores. On the other hand, however, an increase in surface area would also produce a persistent increase in release rate and, in principle, this could occur without opening of closed pores (for example, by intergranular micro-cracking).

Formation of a burst by such a mechanism would require the opening of one pore only or the opening of several over a short period. To assess the feasibility of such behaviour producing bursts of the observed size, the curve in Figure 5 was used to estimate the quantity of gas released in the burst which occurred after 300 minutes annealing. By extrapolating the initial linear portion of the curve, the expected value of f (without burst) was estimated for the next sampling time and subtracted from the observed value to give the contribution of the burst alone. This figure was then used to calculate the actual quantity of Xe-133 in the burst (knowing the total Xe-133 count for the irradiated specimen and the efficiency of the gamma counter (Hanna, Walker and Beach 1967)) and to this was added the quantity of other stable and long-lived fission gases which would also have been present. The total quantity of gas was found to be 7×10^{-16} moles.

Metallographic examination of COP-25-B2 fuel particles (Figure 6) showed that pores of 5 micrometres diameter and less were common. If the calculated quantity of gas released in a burst were contained on one 5 micrometre pore at 1400°C it would be at a pressure of 5×10^6 dyne cm^2 . Assuming the surface energy to be the same as that of UO_2 (650 dyne cm^{-1} , Whapham 1966) the calculated surface tension restraint on the pore could also be 5×10^6 dyne cm^{-2} .

These calculations are only approximate, but they suggest that pores smaller than 5 micrometres in diameter could be unstable and would tend to grow if they contained quantities of gas comparable to those released in mid-anneal bursts. They suggest too, that growth would be slight; hence, of the many pores close to the free surface, relatively few might break through the surface. This is consistent with the requirements for bursts of the size and frequency observed.

The above calculations suggest that it is unlikely that a change in slope without a burst could be explained by successive opening of pores as the increase should be much greater than is observed. Explanation in terms of slow release down a path of interconnected pores would be plausible but, in this case, the increased release rate should have a finite lifetime corresponding to the time taken for the total escape of the gas originally trapped in the pore.

An increase in surface area would, in itself, lead to enhanced release rates by lowering the diffusion distances for release at free surfaces. It does not follow, however, that a burst release would necessarily be followed by a permanently enhanced release, because the increase in surface area associated with the opened pore would be insignificant.

Unfortunately, up to the present time no metallographic evidence of pore growth or micro-cracking has been sought.

The scatter in results at a given temperature for a given batch of particles ($D'_{\text{max}}/D'_{\text{min}}$ in the range 4 to 10) could be due in part to a variable degree of pore growth by the above mechanisms. However, other factors such as inhomogeneity of pore distribution and of U-235 content are also likely to have had an effect.

3.3 Summary of Results on Fuel Particles

As stated in Section 1, the main aim of the work on fuel particles was to compare the fission gas release behaviour of bare fuel particles with that of fuelled BeO spheres. In this context the batches of greatest interest were COP-25-B2 and X-124-3. The release parameters for the two batches were:

COP-25-B2	$9 \times 10^{-12} \text{ sec}^{-1}$	at 1200 °C
	$1.35 \times 10^{-10} \text{ sec}^{-1}$	at 1400 °C
X-124-3	$3 \times 10^{-11} \text{ sec}^{-1}$	at 1200 °C

The release parameter at 1400 °C was not measured for batch X-124-3 but was calculated to be $6 \times 10^{-10} \text{ sec}^{-1}$, assuming an energy of activation comparable with that for COP-25-B2.

4. XENON RELEASE FROM PROTOTYPE FUEL ELEMENTS

4.1 Specimen Details

The fuelled spheres tested in this work included some from each of the four stages described in Section 1. Essential details of specimen type, history and density are given in Table 2. Most contained coarse fuel particles (150 to 200 micrometres) in kernels bonded to the outer unfuelled shell. However, the tests also included four spheres with fine fuel particles (about 5 micrometres) and bonded shells, and two spheres with fine particles, unbonded shells and porous buffer zones between kernels and shells (spheres LH44 and LH45).

The six spheres with identification numbers prefixed by 'X-6' (see Table 2) were prepared in the hope of testing the effect of porosity (or density) by sintering at temperatures of 1450, 1525 and 1700 °C. This was only partly successful, however, as the expected increase of density with temperature was not achieved and a density minimum was encountered at 1525 °C.

Spheres in the LH-series were prepared from two nominally identical batches of Brush UOX beryllium oxide with an addition of 0.1 and 0.2 per cent magnesia to promote sintering. Sintering times of four and six hours were used at temperatures of 1350, 1400, 1450 and 1500 °C.

Specimens LH1 to LH27 contained fuel particles from batch COP-25-B2 which was thoroughly tested in P.A.D. experiments as described in Section 3. Specimens LH30, LH33 and LH34 contained fuel particles from batch X-124-3 which was also thoroughly tested by the P.A.D. method. Although this batch was enriched in U-235 (by a factor of about 29 compared with COP-25-B2) the irradiation time was reduced so that the fission density remained the same as that in spheres containing COP-25-B2 fuel.

Spheres LH38 to LH45 all contained fine fuel particles of an equimolar urania-thoria mixture. Again, the irradiation time was adjusted so that the fission density remained constant.

Specimens LH20 to LH45 had unfuelled coatings 4.6 mm thick. The remainder had coatings 1.3 mm thick.

4.2 Release of Xe-133

Release rate parameters measured on the fuelled spheres are listed in Table 2. Within the range of sensitivity of the P.A.D. technique the release parameter could not be correlated with any of the fabrication variables. Instead the results fell into two broad groups, one in which the parameters were high, in most cases too high to measure because of the copious release of activity, and one in which the parameters were below or just approached the limit of sensitivity.

In general, the results were very encouraging and demonstrated that BeO coatings can very markedly reduce the escape of fission products. Of the forty spheres tested, twenty-seven gave release parameters of $8 \times 10^{-17} \text{ sec}^{-1}$ or less; of these, twenty released so little Xe-133 that parameters could not be determined and it can be said only that they were less than $10^{-17} \text{ sec}^{-1}$.

Twenty-four spheres containing fuel particles from batch COP-25-B2 were tested. Seventeen had release parameters of $8 \times 10^{-17} \text{ sec}^{-1}$ or less, which is an improvement of six or more orders of magnitude over the parameters for bare fuel at the same temperature. Remembering that the quantity released is proportional to the square root of D , the reduction in quantity of xenon released is by at

least three orders of magnitude. Similarly, for the three spheres containing X-124-3 fuel particles, the parameters are over seven orders of magnitude lower than that for the bare fuel. (This fuel was not tested at 1400 °C; the above estimate is based on a value of $6 \times 10^{-10} \text{ sec}^{-1}$ calculated from the 1200 °C value assuming an energy of activation similar to that for COP-25-B2 and X-124-1,2).

No positive explanation is available of the high xenon releases from several of the spheres. It seems highly probable, however, that it is due to porosity, micro-cracks or even small macro-cracks which could not be detected by the dye penetrant method used. One sphere, LH13, broke into several pieces as it was being drawn slowly into the hot zone of the furnace. Several others which gave negligible releases throughout the whole anneal were subsequently water quenched from about 200 °C; in each case they gave a high xenon release when re-annealed although no cracks could be detected by dye penetration; nevertheless there is little doubt that cracking was the reason for the high xenon releases. It could well be, therefore, that other spheres which showed high fission gas permeabilities were also cracked.

It is interesting, though perhaps not significant because of the small number of specimens involved, that of the four fine dispersion spheres sintered at 1400 °C, the two with porous buffer zones released very little Xe-133 whereas the two without released large amounts. Possibly the buffer zone improved the thermal shock resistance of the spheres to a point where the whole sphere or, at least, the dense outer shell, remained uncracked; however the poor behaviour of the spheres without buffer zones cannot be attributed positively to cracking. Reeve (private communication) has shown that the fuel-BeO mixture used in these specimens had a lower shrinkage on sintering than the pure BeO in the outer shell, but metallographic examination of a control sample from the same batch as LH40 and LH41 failed to show cracks in the cladding. The possibility remains, however, that cracking occurred during heating for the P.A.D. anneal.

5. DISCUSSION

These experiments have demonstrated that BeO based, BeO clad fuel elements can be made highly fission product retentive at low burnup. The results have also indicated the value of the P.A.D. technique as a means of selecting the best materials for testing by the more rigorous, but expensive and time consuming, in-pile methods.

The major value of the results lies in the comparison of the behaviour of fuelled spheres and bare fuel particles, and it is of interest to extrapolate them to the in-pile, high temperature behaviour of the spheres. It can be assumed with reasonable confidence that any observed difference between two specimens in P.A.D. experiments would be reflected in in-pile behaviour, provided neutron irradiation had a similar effect on diffusion in both specimens. In Section 4.2 it was stated that a difference by a factor of 10^6 in release parameter is equivalent to a factor of 10^3 in the actual xenon release rate. Thus, it can be predicted that the in-pile R/B ratio (ratio of release rate to birth rate) of the ABORIGINE fuel elements will be at least three orders of magnitude lower than that for the bare fuel particles. In-pile experiments to be reported have shown that the Xe-133 release parameters for bare fuel particles (batches X-124-1,2 and COP-25-B2) are about 10^{-3} at 800 °C with little or no temperature dependence up to that temperature. Assuming that a similar value holds for 1000 °C, the expected R/B ratio for a fuelled sphere would be no higher than about 10^{-6} .

A current series of in-pile experiments using specimens selected on the basis of the P.A.D. results will be reported elsewhere but it can be stated that release parameters of $R/B = 10^{-7}$ have been measured at 1000 °C. This is in good agreement with the above estimate from P.A.D. results. Hanna, Walker and Reeve (A. A. E. C. unpublished report) have estimated that a maximum value of 5×10^{-6} is required for the safe operation of ABORIGINE. Hence, it appears that the prototype elements tested in this work would meet this requirement at least at low burnup and low fast neutron doses.

6. CONCLUSIONS

It has been demonstrated that dispersion type fuel elements utilising a beryllium oxide matrix and beryllium oxide cladding can be highly fission product retentive when compared with the bare con-

stituent fuel particles. The magnitude of the improvement is such as to suggest that in-pile behaviour, at low burnup at least, will be adequate for a small, open cycle reactor of the ABORIGINE type.

The work described has also shown that the post-activation diffusion technique based on the equivalent sphere model is a very useful sorting test despite the limitations of the model in its simplest form.

7. REFERENCES

- Belle, J. (Editor) (1961). – Uranium Dioxide; Properties and Nuclear Applications. U.S.A.E.C. Naval Reactors, Division of Reactor Development.
- Booth, A.H. (1957). – CRDC-721.
- Cohen, I. and Berman, R.M. (1966). – J. Nuc. Mat. 18: 77.
- Davies, D. and Long, G. (1963). – AERE-R4347.
- Frigerio, G. and Gerevini, T. (1965). – J. Nuc. Mat. 16: 76.
- Hanna, G.L., Walker, D.G. and Beach, P.M. (1967). – AAEC/TM384.
- Hickman, B.S., Rotsey, W.B., Hilditch, R.J. and Veevers, K. (1968). – J. Am. Ceram. Soc., 51 (2): 63.
- MacEwan, J.R. and Stevens, W.H. (1964). – J. Nuc. Mat. 11: 77.
- Reeve, K.D., Clare, T.E., Silver, J.M. and Bridgeford, K.C. (1966). – AAEC/TM333.
- Toner, D.F. and Scott, J.L. (1961). – ORNL-3142.
- Walker, D.G. and Hickman, B.S. (1967). – J. Nuc. Mat. 24: 60.
- Whapham, A. (1966). – Nuc. Appl. 2: 123.

TABLE 1

SUMMARY OF Xe-133 RELEASE PARAMETERS AND FABRICATION HISTORIES FOR URANIA-THORIA FUEL PARTICLES

Fabrication Step	COP-25-B2	COP-17-B1	COP-17-B2A	COP-17-B2B	X-124-1,2	X-124-3
Co-precipitate Th(OH) ₂ and ADU	Yes IU : 10 Th	Yes IU : 12.5 Th	Yes IU : 12.5 Th	Yes IU : 12.5 Th	Yes IU : 10.5 Th	Yes IU : 9.8 Th
Grind precipitate	No	No	No	No	2 hours, wet	No
Air dry, 85 °C	Yes	Yes	Yes	Yes	Yes	Yes
Dry grind	Yes	Yes	Yes	Yes	No	Yes
Calcine in H ₂ at 700 °C	Yes	No	Yes	Yes	Yes	No
Grind	No	No	No	Yes, dry	Yes, wet	No
Isopress at 17 - 20 TSI	Yes	Yes	Yes	Yes	Yes	Yes
Crush and seive to 250-300 μm	Yes	Yes	Yes	Yes	Yes	Yes
Sinter, 1700 °C for 2 hours in H ₂	Yes	Yes	Yes	Yes	Yes	Yes
Bulk density of particles (g cm ⁻³)	8.9	9.5	9.5	9.3	9.4	9.9
Mean grain size (μm)	20	ND*	10.1	10.4	4 - 7	13 - 100
Mean D ¹ at 1200 °C (sec ⁻¹)	9 x 10 ⁻¹²	1.4 x 10 ⁻¹⁰	3.5 x 10 ⁻⁹	5.7 x 10 ⁻¹⁰	5.4 x 10 ⁻¹¹	3.2 x 10 ⁻¹¹

* Not Determined

TABLE 2

SUMMARY OF Xe-133 RELEASE PARAMETERS FOR PROTOTYPE BeO BASED FUEL ELEMENTS FOR THE ABORIGINE REACTOR

Sphere No.	BeO Coating Thickness (mm)	Vol.% (U, Th)O ₂ in core	U : Th ratio (atoms)	Fuel Particle Batch	Porous Buffer Zone	MgO added to BeO (%)	Sintering Temp. (°C)	Density (g cm ⁻³)	Annealing Temp. (°C)	D' (sec ⁻¹)
X-6-A-22	1.1 - 1.4	1.7	1 : 10	X-6	No.	-	1450	3.023	1200	1.4×10^{-16}
X-6-A-23	"	"	"	"	"	-	"	3.024	1400	4×10^{-17}
X-6-B-17	"	"	"	"	"	-	1525	3.010	1200	2.1×10^{-17}
X-6-B-19	"	"	"	"	"	-	"	3.005	1400	High*
X-6-C-12	"	"	"	"	"	-	1700	3.049	"	6.7×10^{-15}
X-6-C-13	"	"	"	"	"	-	"	"	"	$< 10^{-17} \dagger$
LH 1	"	2.63	"	COP-25-B2	"	0.2	1400	2.98	"	$< 10^{-17}$
LH 2	"	"	"	"	"	"	1500	2.99	"	High
LH 3	"	"	"	"	"	"	1575	2.93	"	"
LH 4	"	"	"	"	"	"	1400	3.02	"	High**
LH 5	"	"	"	"	"	"	"	3.07	"	"
LH 6	"	"	"	"	"	"	"	ND ^{††}	"	$< 10^{-17}$
LH 7	"	"	"	"	"	"	1350	3.01	"	High
LH 8	"	"	"	"	"	"	1450	3.05	"	"
LH 9	"	"	"	"	"	"	"	3.04	"	1.8×10^{-17}
LH10	"	"	"	"	"	"	"	3.05	"	$< 10^{-17}$
LH11	"	"	"	"	"	"	"	3.06	"	$< 10^{-17}$
LH12	"	"	"	"	"	"	"	3.00	"	$< 10^{-17}$
LH13	"	"	"	"	"	"	1400	2.95	"	- †
LH14	"	"	"	"	"	"	1500	3.04	"	9.5×10^{-16}
LH15	"	"	"	"	"	"	1400	2.98	"	3.3×10^{-17}
LH16	"	"	"	"	"	"	1450	2.96	"	8×10^{-17}
LH17	"	"	"	"	"	"	"	3.04	"	7.3×10^{-17}
LH18	"	"	"	"	"	"	1500	3.06	"	$< 10^{-17}$

LH19	"	"	"	"	"	"	1400	3.01	"	1 x 10 ⁻¹⁷
LH20	4.5-4.75	5	"	"	0.1	"	1450	3.00	"	6 x 10 ⁻¹⁷
LH22	"	"	"	"	"	"	"	3.02	"	< 10 ⁻¹⁷
LH23	"	"	"	"	"	"	"	"	"	"
LH24	"	"	"	"	"	"	"	3.01	"	"
LH25	"	"	"	"	"	"	"	3.00	"	"
LH27	"	"	"	"	"	"	"	2.99	"	"
LH30	"	"	"	X-124-3	"	"	"	ND ††	"	"
LH33	"	"	"	"	"	"	1400	3.04	"	"
LH34	"	"	"	"	"	"	"	3.01	"	"
LH38	"	2.06	1:1	Fine	"	"	1450	2.92	"	"
LH39	"	"	"	"	"	"	"	"	"	"
LH40	"	"	"	"	"	"	1400	2.94	"	High
LH41	"	"	"	"	"	"	"	"	"	"
LH44	"	"	"	"	Yes	"	"	2.91	"	< 10 ⁻¹⁷
LH45	"	"	"	"	"	"	"	2.94	"	"

* 'High' means X-133 release too great for measurement of D'

† D' = 10⁻¹⁷ sec⁻¹ represents limit of sensitivity

** LH4 : D' < 10⁻¹⁷ sec⁻¹ for first eight hours of anneal

† LH13 disintegrated on raising into furnace

†† ND Not Determined

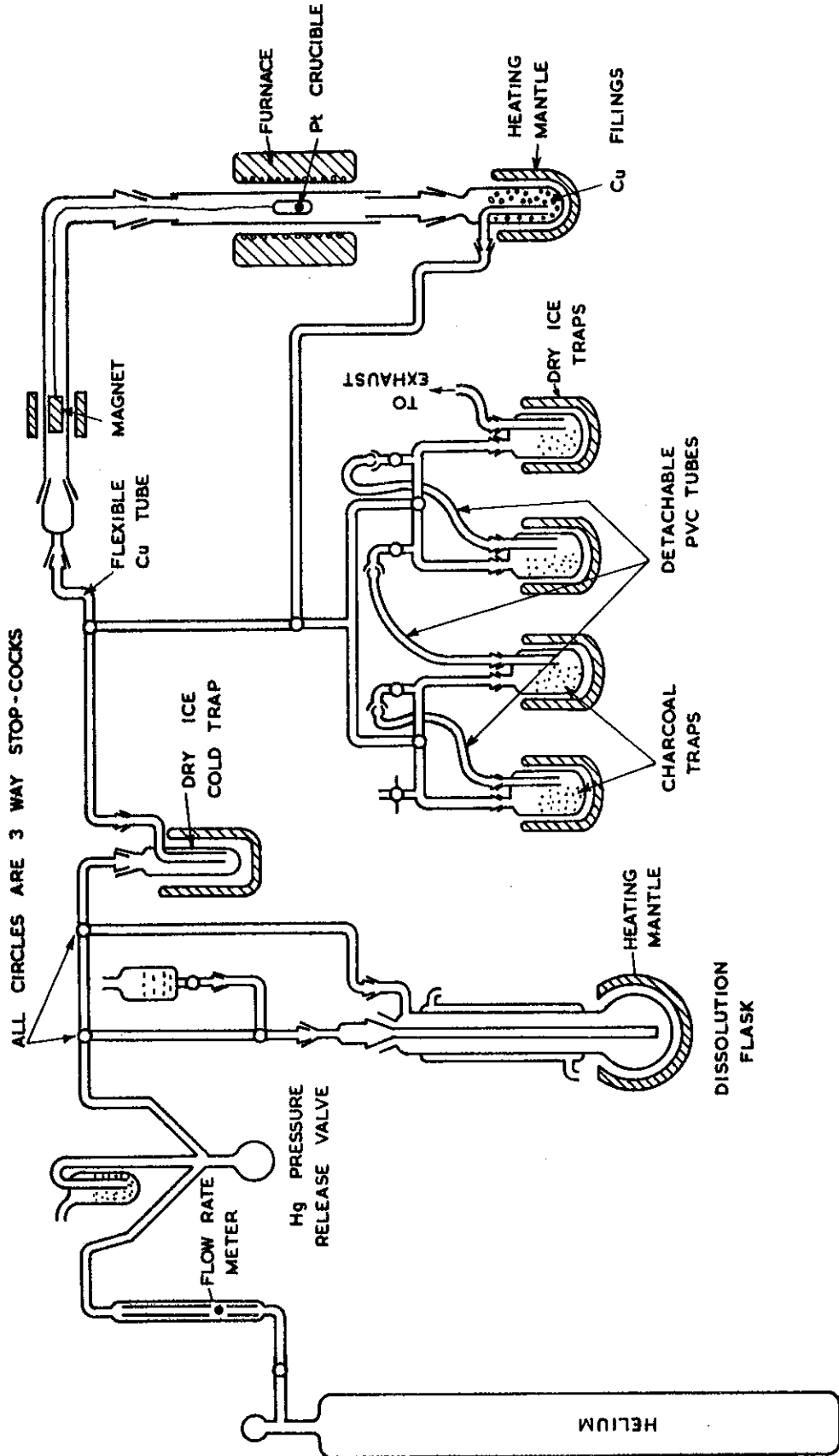


FIGURE 1. DIAGRAM OF APPARATUS FOR POST-ACTIVATION DIFFUSION EXPERIMENTS

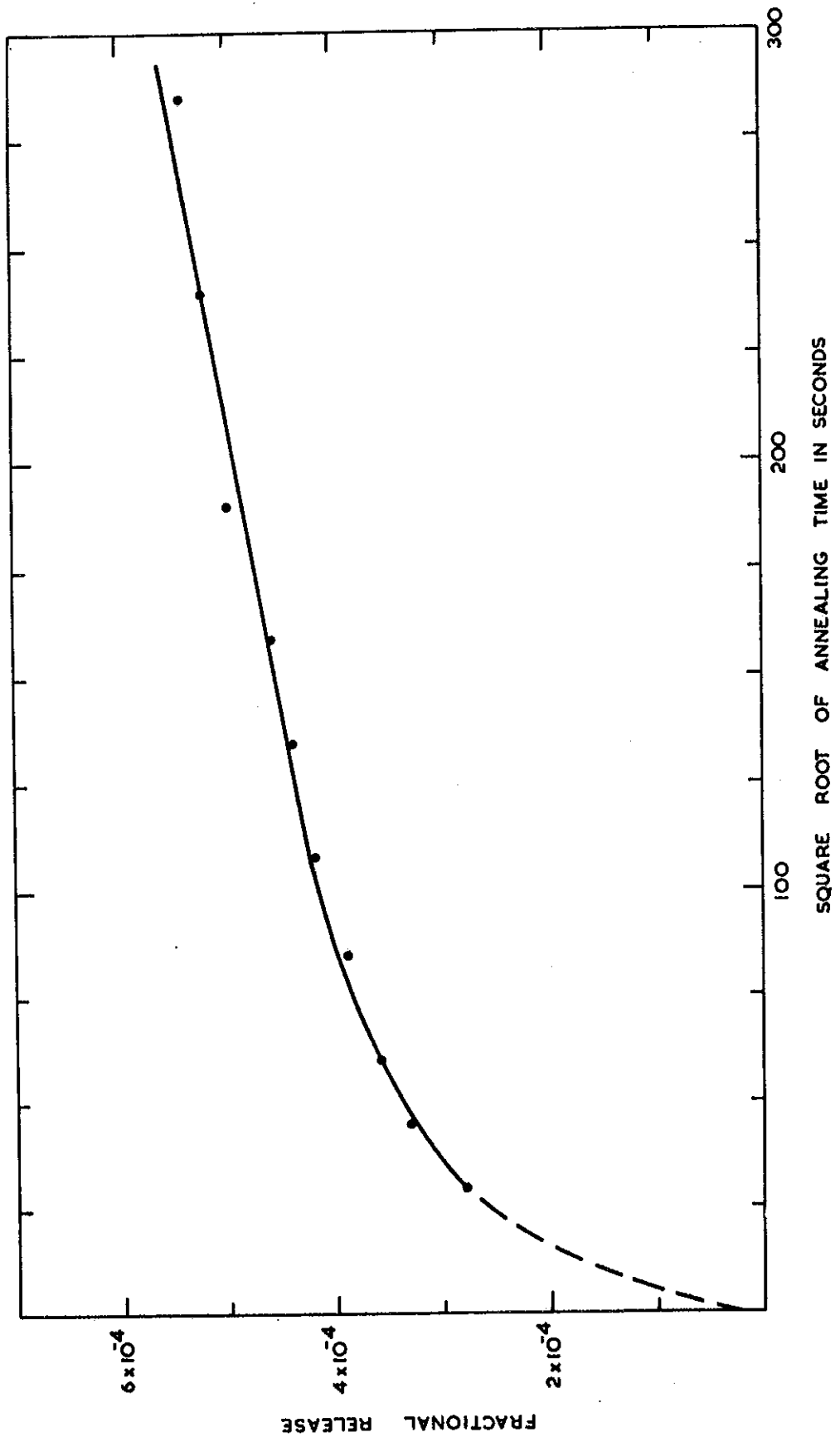


FIGURE 2. DIFFUSION CURVE FOR COP-25-B2 FUEL PARTICLES AT 1000°C

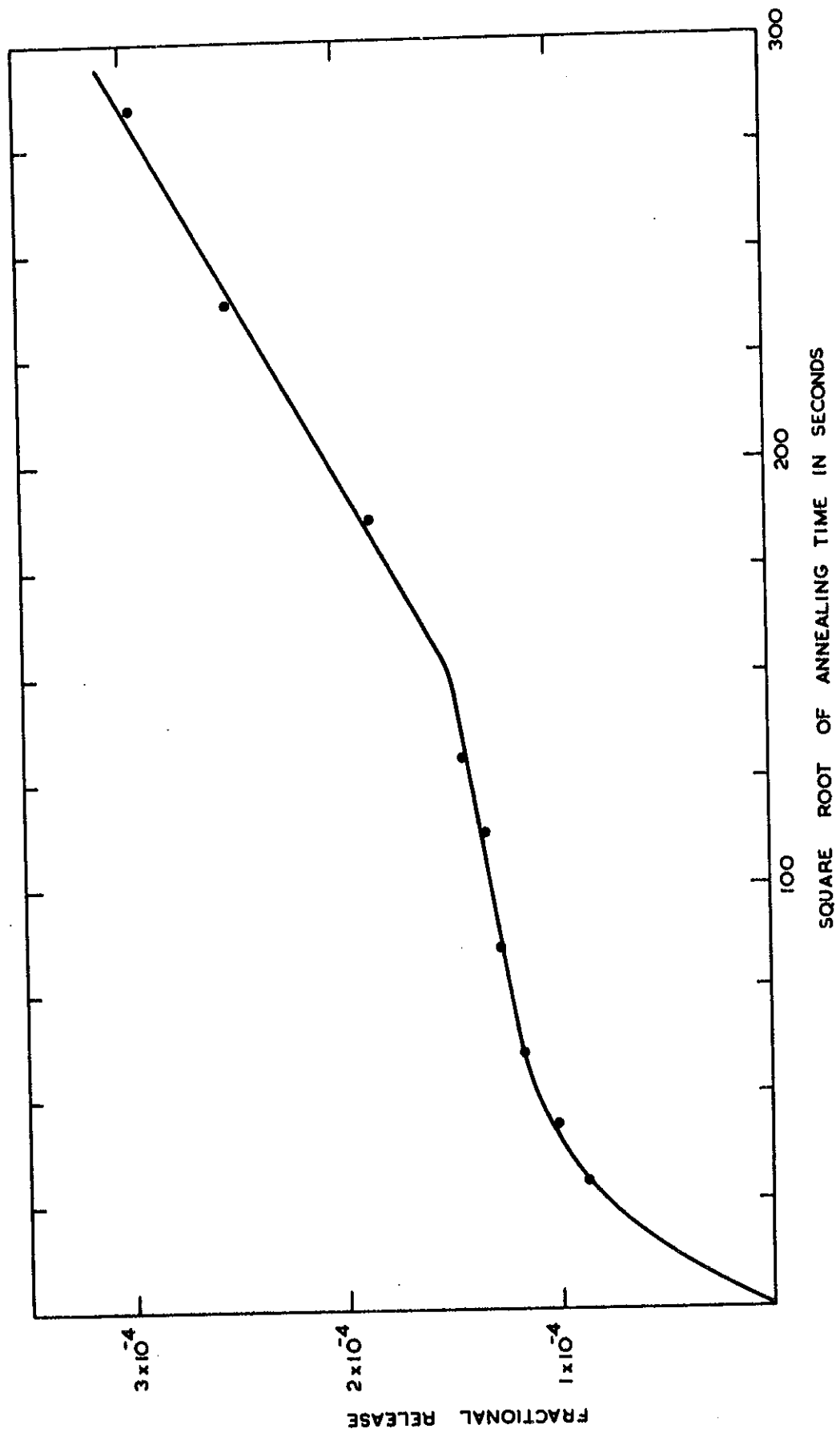


FIGURE 3. DIFFUSION CURVE FOR COP-25-B2 FUEL PARTICLES AT 1400°C

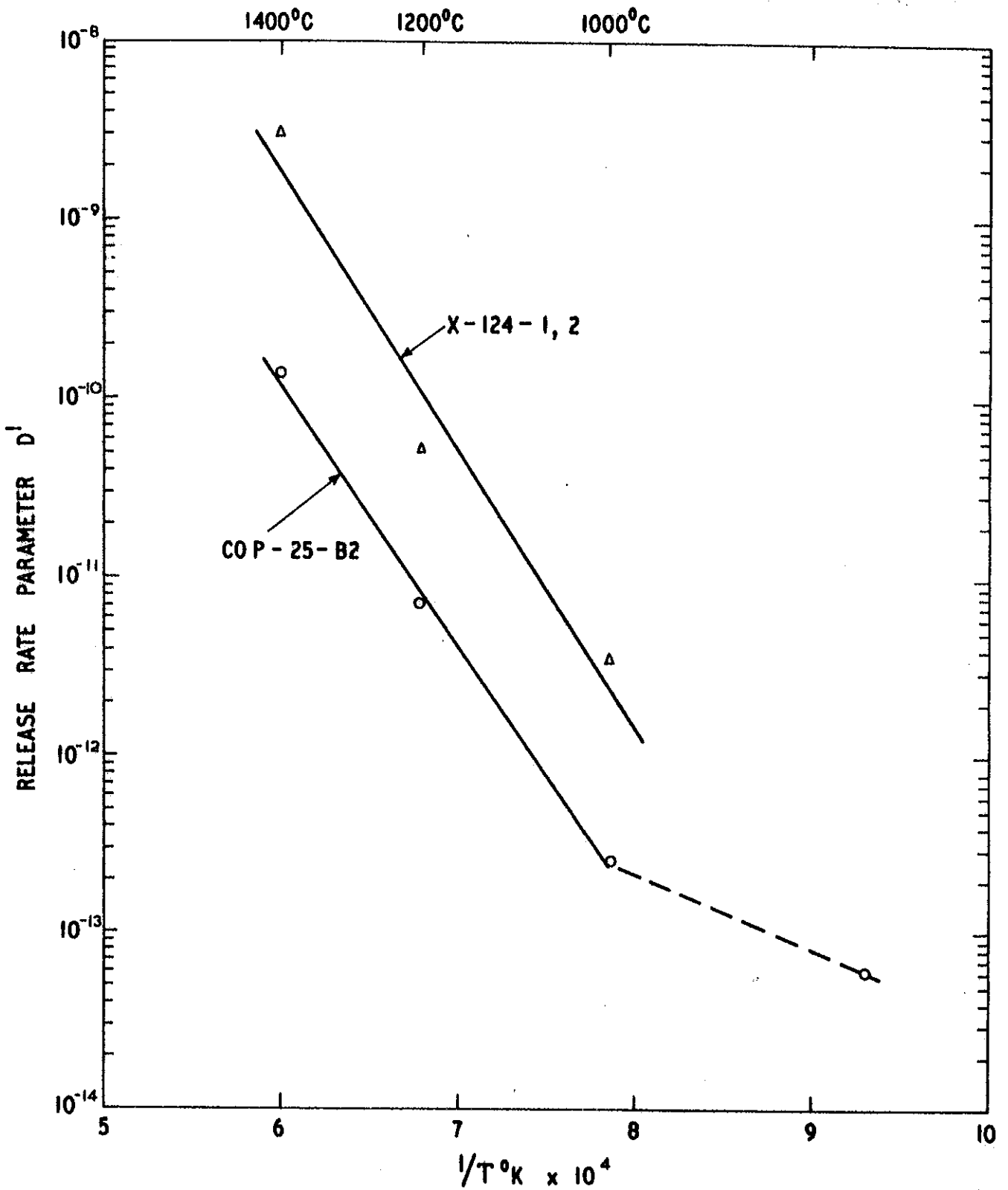


FIGURE 4. ARRHENIUS PLOTS OF RELEASE PARAMETERS OBTAINED FOR FUEL PARTICLES

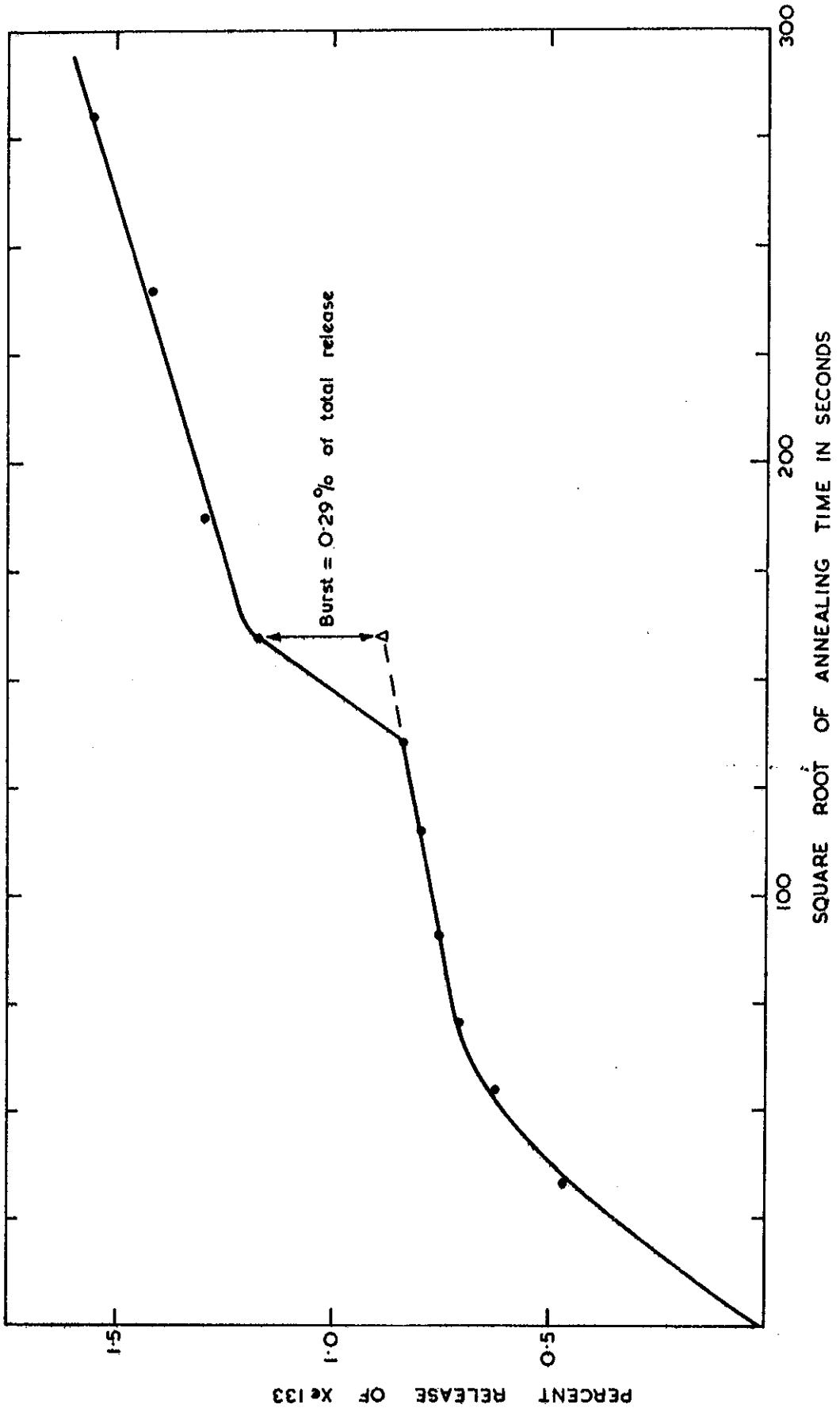
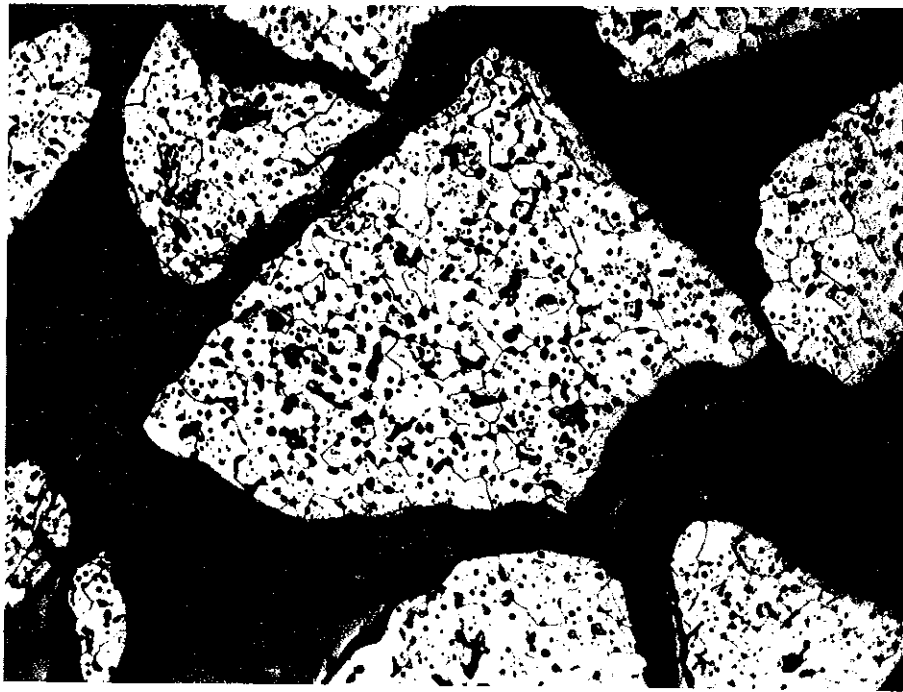


FIGURE 5. DIFFUSION CURVE FOR FUEL PARTICLES, SHOWING A MID-ANNEAL 'BURST'



X250

**FIGURE 6. PHOTOMICROGRAPH OF URANIA-THORIA FUEL
PARTICLES FROM BATCH COP-25-B2**